Compact Wideband Quad-Element MIMO Antenna with Reversed S-Shaped Walls

Fei Wang[*]**, Shifeng Li, Qing Zhou, and Yubin Gong**

Abstract—We propose a compact wideband planar quad-element multiple input, multiple output (MIMO) antenna, which can cover a wide bandwidth ranging from 2.2 to 30 GHz. Novel reversed S-shaped walls provide high isolation between antenna elements within an extremely closed space, with the edge-to-edge distance between elements being only 1 mm. The simulated and measured results with respect to S parameters and radiation patterns are in good agreement. The experimental results indicate that the quad-element MIMO antenna can provide wide bandwidth (2.2–30 GHz), high isolation (with the transmission coefficients below -19 dB), and low profile (only $\sim \lambda_0/40$) within a compact structure (32 mm $\times$ 32 mm $\times$ 4.5 mm). This compact wideband quad-element MIMO antenna with high isolation and low profile has important applications in mobile devices or other small-scaled equipment in future 5G communication.

1. INTRODUCTION

With the continuous development of mobile communication and the urgent demand for high data rate, stable communication quality, low latency round-trip time, the fifth generation (5G) cellular communication has become one of the topical research areas in the worldwide mobile communication scenario [1, 2]. Attaining wider communication bandwidths is the need of the hour to meet this demand. The lower frequency bands, especially below 3 GHz, is fulfilled with the existing communication systems. Therefore, the shortage of communication frequency bands at the lower frequency end has led to looking at higher frequency bands above 6 GHz, even up to the millimeter-wave frequency band [3–5]. The exploration of sub-6-GHz spectrum is also being carried out for long range communication. Thus, the 5G communication covers the range of frequencies extending from 3 to 30 GHz, even higher up to ~ 60 GHz [6–8].

As one of the most important technologies in the 5G communication, multiple input, multiple output (MIMO) antenna technology, which has been applied in digital television, wireless local area network, metropolitan area network, and mobile communication, can effectively improve data transmission ratio and communication quality. The isolation between antenna elements is considered as one of the most important parameters to estimate the MIMO antenna performance. In recent years, some concepts such as slots, electromagnetic band gaps, resistive walls, and artificial magnetic conductors have been used to realize high isolation in MIMO antennas [9–12]. However, the implementation of concept still faces problems such as narrow operation bandwidth (from 10 to 30% relative bandwidth), large scale (of total length of $\sim \lambda_0/2$ to $\sim 2\lambda_0$, λ_0 referring to the wavelength corresponding to the lowest operation frequency), and high profile ($\sim \lambda_0/6$ to $\sim \lambda_0/2$).

Hence, driven by these urgent demands, the studies of ultra-wideband (UWB) antennas have been carried out worldwide. Many efforts have been made for achieving wide operation band such as slots [13], parasitic elements [14], log-periodic [15], fractal geometry [16], and metamaterials [17, 18]. Furthermore,

the MIMO technology is introduced into wideband antenna systems [19, 20], in which the techniques mentioned above are used for enhancing the isolation. So far, the efforts to reduce the overall size and enhance the isolation have been continuing.

Therefore, in this paper, to alleviate the above problems, we propose a compact wideband quad-element MIMO antenna with reversed S-shaped walls (RSWs). In Section 2, the design of an elliptic monopole antenna, with due care to optimize it for wide operating band, is presented. In Section 3, the development of the quad-element MIMO antenna is described while proposing the introduction of an RSW in the design for broadband decoupling. In Section 4, the quad-element MIMO antenna with four RSWs is fabricated and measured. Finally, in Section 5, the major findings of the work are highlighted and summarized.

2. SINGLE WIDEBAND ANTENNA DESIGN

The elliptic monopole antenna with coplanar waveguide (CPW) feed line, which is shown in the left of Fig. 1(a), is printed on an FR-4 substrate (relative permittivity = 4.4, loss tangent = 0.06, and thickness = 1 mm). The CPW structure includes a strip line of 1 mm width and two gaps of 1 mm width. The two holes on the substrate are used for assembling with the K-type connectors. Using HFSS, the simulated S_{11} parameter of the monopole antennas is presented in Fig. 1(b). Clearly, the single-ellipse monopole antenna does not have good impedance matching at multiple frequencies, typically, ~ 4 and ~ 10 GHz (Fig. 1(b)).
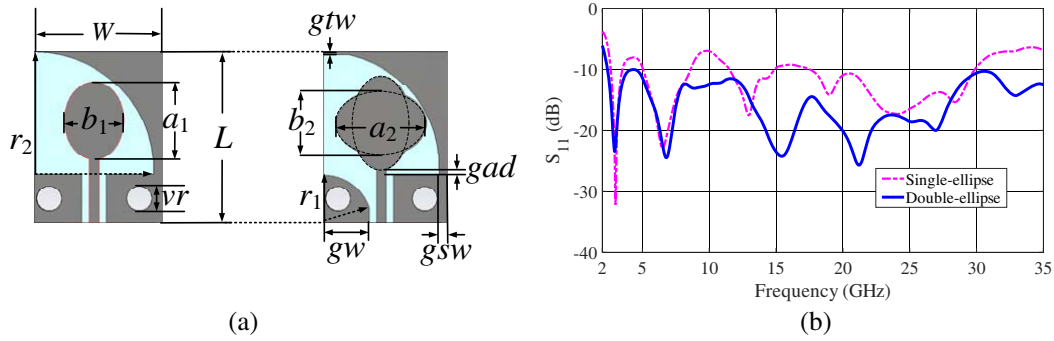

Figure 1. (a) Dimensional parameters of single-ellipse and double-ellipse antennas and (b) their HFSS-simulated S_{11} parameters.

In order to further extend the operation bandwidth, another ellipse antenna with orthogonal major axes is added without changing the overall size of the antenna. Since the axe length of the second ellipse is close to the first one, it can improve the impedance matching at similar frequencies, for instance, ~ 7 GHz and 14 GHz.

Besides, we have also optimized the ground plane structure. A rectangle patch of 0.3 mm width is added on top of the ground plane, and the left ground plane is replaced with an arc. The final geometry of the wideband antenna is illustrated in the right portion of Fig. 1(a), and the dimensional parameters are listed in Table 1. The length of the arc on the left ground plane is about 8.2 mm which is of the order of (1/4)th of the wavelength corresponding to 8 GHz operating frequency. The calculated radius of arc on the right ground plane $r_2 = W - gsw = 12$ mm and arc length = 18 mm, with the latter being of the order of wavelength corresponding to 11 GHz. The two arcs enhance the resonances at the corresponding two frequencies, which lead to the two valleys of S_{11}, as shown in Fig. 1(b). Hence, the compact wideband double-ellipse antenna can operate from 2.4 to 30 GHz.

To validate our design, we have fabricated the compact wideband double-ellipse antenna as shown in the perspective-inset of Fig. 2. The measured S_{11} parameters of the fabricated antenna are compared with the simulated ones, as illustrated in Fig. 2. Even though the fabrication errors can lead to impedance mismatch at higher frequencies, the antenna can operate from 2.4 to 30 GHz (Fig. 2), which can meet the requirements for the 5G communication and other communication systems such as Bluetooth and WLAN.

Table 1. Dimensions in mm of the proposed antenna.

| W	L	r_1	vr	a_1	b_1
13	18	5	2	10	6
a_2	b_2	gw	gsw	gtw	gad
9.4	6.8	4.5	1	0.3	0.2
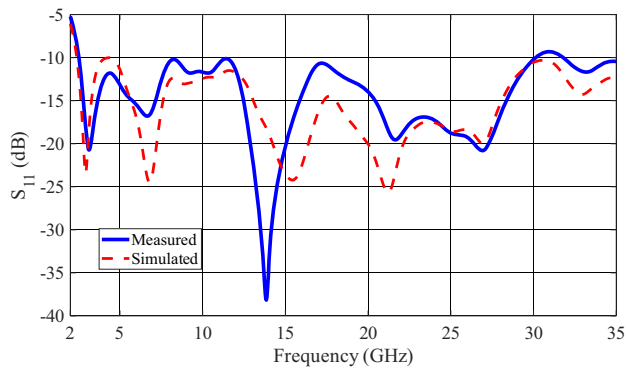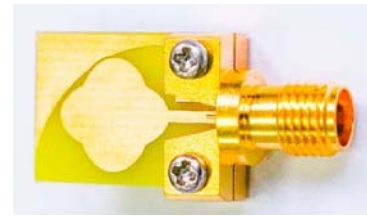
(a) (b)

Figure 2. (a) Simulated and measured S_{11} parameters of the compact double-ellipse wideband antenna, and (b) the fabricated antenna sample.

3. MIMO ANTENNA DESIGN

Based on the work presented in Section 2, we have developed a quad-element MIMO antenna. The antenna consists of four elements in which every two adjacent elements are orthogonally placed with the distance $ad = 1$ mm between them (Fig. 3(a)). Subsequently, we have used HFSS to simulate the S parameters of this MIMO antenna (Fig. 3(b)). Due to the extended ground plane, the lowest operating frequency is extended from 2.4 to 2.2 GHz. At frequencies above 5 GHz, the S_{21} parameter maintains its value under -20 dB, thereby providing an adequate isolation between two antenna elements. However, the S_{12} parameter continuously increases as the frequency decreases from 5 GHz. This is attributed to the distance relative to wavelength between antenna elements becoming shorter with longer wavelengths
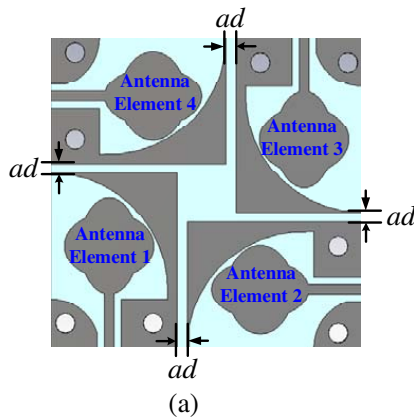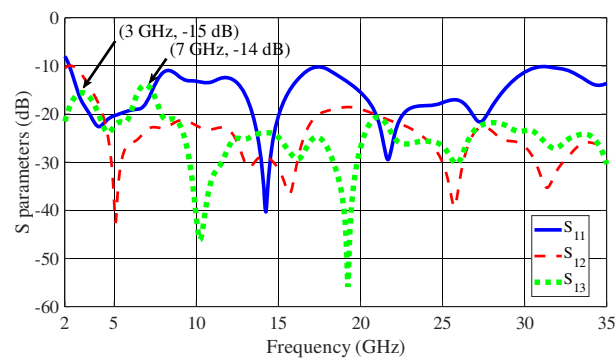
(a) (b)

Figure 3. (a) Geometry showing the orthogonal element pairs; and (b) S parameters of the quad-element MIMO antenna obtained by HFSS simulation.
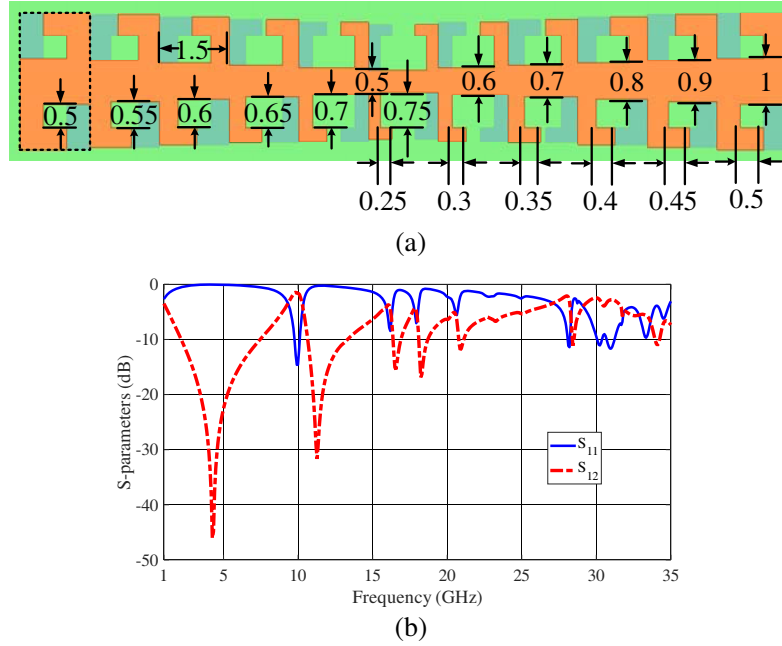
(a)

(b)

Figure 4. (a) Geometry of RSW (with its dimensions given in mm) and (b) its S parameters.

causing a stronger mutual coupling at lower frequencies. Besides, the S_{13} parameter reaches -15 dB and -14 dB at ~ 3 GHz and ~ 7 GHz, respectively. These findings have pointed out that the isolation needs to be enhanced in the range from 2.2 to 7 GHz, which prompted us to introduce a decoupling structure in the design for enhancing the isolation.

Considering the space of only 1 mm $\times$ 18 mm available between antenna elements, we have opted to build a 'decoupling wall' instead of etching the decoupling structures on the ground plane. Moreover, since the wavelength corresponding to the frequency 2.2 GHz is $\sim$136 mm, the traditional metamaterial cannot be used here since this would bring a high profile and result in a narrow resonant bandwidth, which cannot meet the demand of broadband decoupling.

Therefore, here we propose an RSW, shown in Fig. 4(a), as the decoupling structure in a compact configuration that can provide a broad bandwidth. The structure consists of an array of reversed S-shaped structures of uniform width 1.5 mm with the remaining structure dimensions gradually tapered (Fig. 4(a)). The same structure with contra-orientation (shown in gray in Fig. 4(a)) is printed on the other side of substrate of 1 mm thickness made of FR-4. Using HFSS, the simulated S parameters of RSW are found as shown in Fig. 4(b). It shows that the designed RSW resonates from 2 to 6 GHz. RSWs with the overall size of 3.5 mm $\times$ 17 mm is placed on the slot between antenna elements as shown in Fig. 5(a). Obviously, the profile (only $\lambda_0/40$) is much lower than that in [9, 10].

Next, after placing RSWs on the slots between antenna elements, the surface current distribution at 3.5 GHz is found, as shown in Fig. 5(a). It clearly shows that the coupling energy is radiated mainly through the top side of the ground plane and exhibits a strong resonance on RSWs. Therefore, the energy coupled to other elements becomes largely reduced. The simulated S parameters of the quad-element MIMO antenna are presented in Fig. 5(b). At ~ 3.5 GHz, the S_{12} parameter of the antenna significantly drops from -15 to -45 dB, and the S_{12} and S_{13} parameters take on values below -19 dB from 2.2 to 30 GHz (Fig. 5(b)).

4. EXPERIMENT AND DISCUSSION

With a view to further validate the characteristics of the proposed quad-element MIMO antenna, it is fabricated as shown in Fig. 6(a). The measured S parameters are illustrated in Fig. 6(b). Due to the symmetry of the structure, the parameter S_{14} is nearly the same as the parameter S_{12}. Thus, the
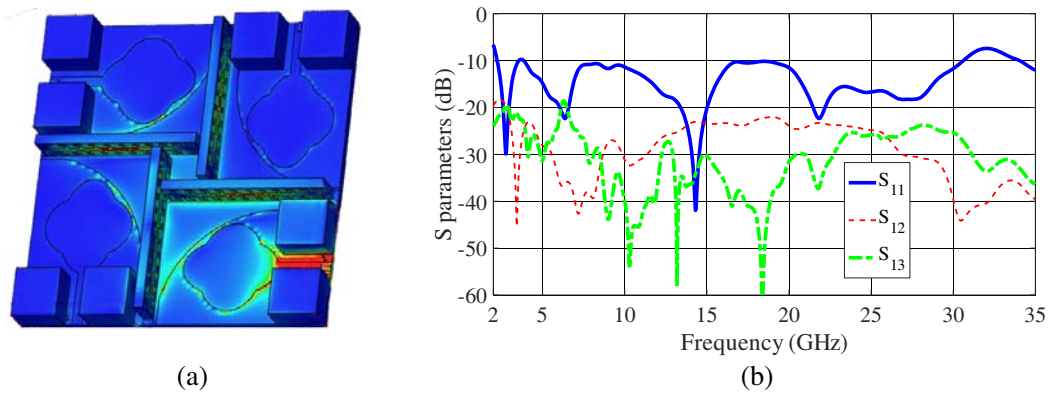
(a)   (b)

Figure 5. (a) Current distribution and (b) S parameters of the quad-element MIMO antenna with RSW.
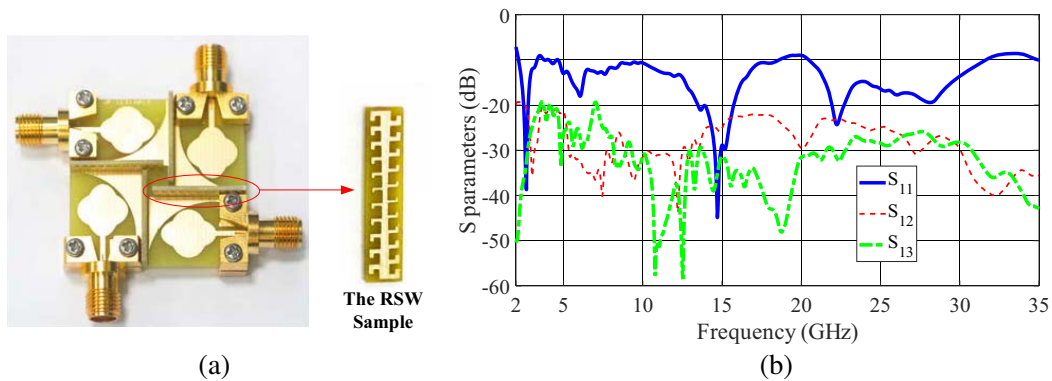

(a)   (b)

Figure 6. (a) Fabricated quad-element of MIMO antenna and (b) measured S parameters.

proposed quad-element MIMO antenna can operate from 2.2 to 30 GHz, and the measured isolation becomes high enough below -20 dB (Fig. 6(b)). Further, the transmission significantly decreases at the central resonant frequency (3.5 GHz) of RSW. Also, due to the reflection at RSW, the S_{11} parameter increases at ~ 3.5 GHz though it is still below -10 dB (Fig. 6(b)).

Figure 7 shows the measured radiation patterns of the proposed quad-element MIMO antenna at 6 and 28 GHz. Thus, we find that the proposed quad-element MIMO antenna has an approximate omnidirectional radiation property which is similar to that of a conventional monopole antenna. Also, there is a significant valley of measured data observed at ~ 90 degrees, which is caused by the influence of the feeding cable (Fig. 7).

The measured radiation efficiency and gain of the MIMO antenna with RSW are presented in Figs. 8(a) and (b), respectively. The radiation efficiency is over 50% in most of the operation band. However, at frequencies under 4 GHz, the radiation efficiency dramatically decreases due to the limitation of the overall size of the proposed MIMO antenna. Similarly, the maximum gain is over 2 dBi in most of the operation band and over 4 dBi at frequencies above 17 GHz. Due to the minimization of the proposed antenna, the maximum gain is quite low at lower frequencies. Note that there is a small valley at ~ 12 GHz which is caused by the non-ideal impedance matching at ~ 12 GHz as shown in Fig. 1(b).

The merit of the proposed quad-element MIMO antenna over some other typical compact quad-element MIMO antenna counterparts reported in references with respect to bandwidth and isolation is highlighted in Table 2. Since our proposed RSW can realize broadband decoupling within an extremely small space, the high isolation is obtained without sacrificing the overall size of the MIMO antenna. Therefore, the proposed quad-element MIMO antenna shows merits such as compactness, wide bandwidth, and high isolation.
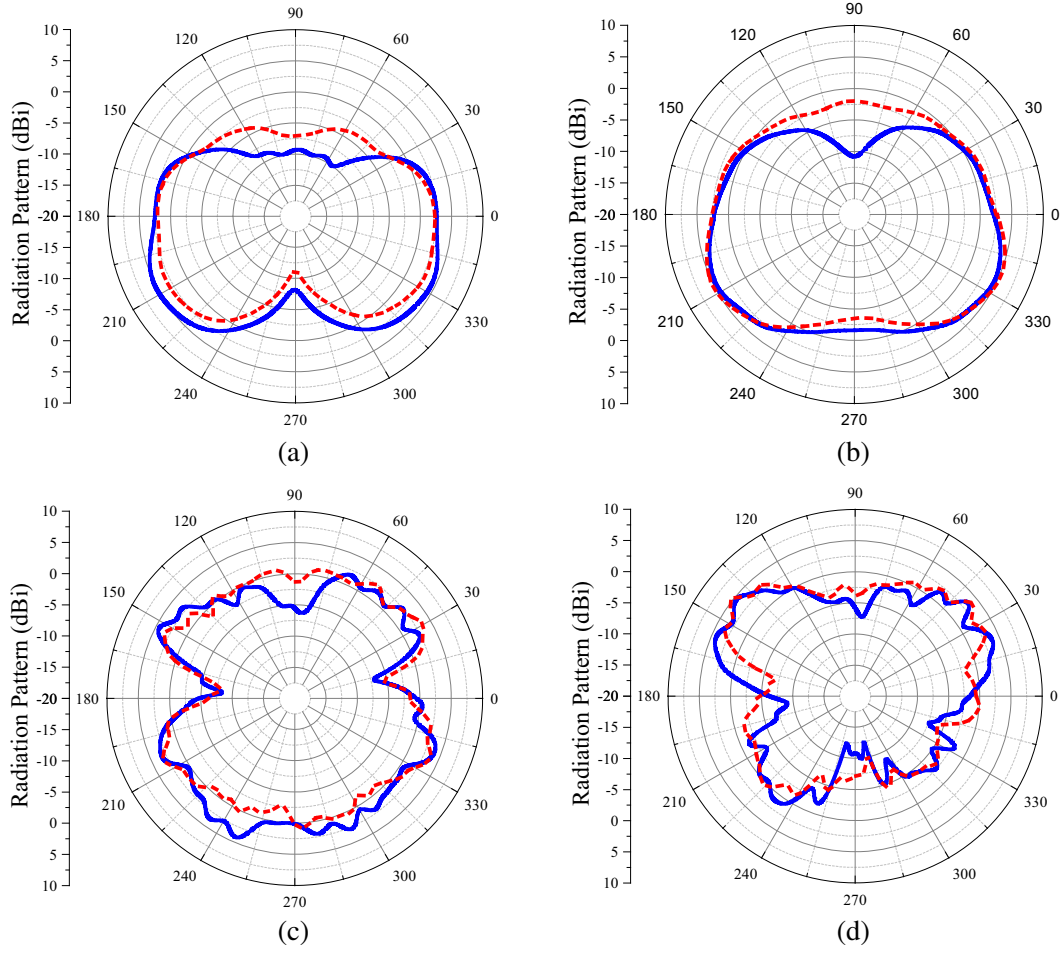
Figure 7. (i) Radiation patterns of the quad-element MIMO antenna on *xoy*-plane (a) and *xoz*-plane (b) at 6 GHz; (ii) and radiation patterns on *xoy*-plane (c) and *xoz*-plane (d) at 28 GHz. The blue solid line and the red broken line refer to the measured and simulated data, respectively.
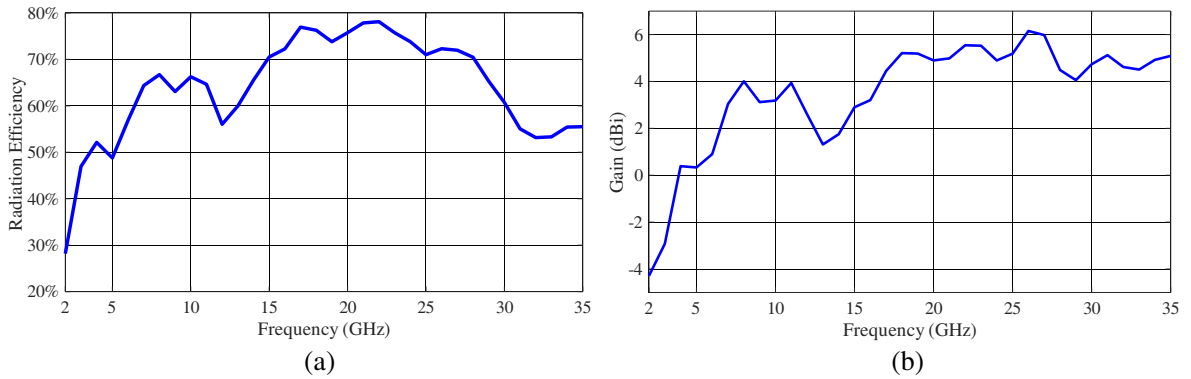

Figure 8. Measured radiation efficiency (a) and gain (b) of the MIMO antenna with RSW.

Furthermore, the enveloped correlation coefficient (ECC) is yet another important parameter to characterize the performance of a MIMO antenna system. The value of ECC, calculated by using the Equation (1) proposed in [26], is found to get reduced significantly around 3.5 GHz after the

incorporation of RSW in our proposed antenna (Fig. 9).

$$\rho_e = \frac{\left| \iint_{4\pi} \left[\vec{E}_1(\theta, \phi) \cdot \vec{E}_2(\theta, \phi) \right] d\Omega \right|^2}{\iint_{4\pi} \left| \vec{E}_1(\theta, \phi) \right|^2 d\Omega \iint_{4\pi} \left| \vec{E}_2(\theta, \phi) \right|^2 d\Omega} \tag{1}$$

Moreover, the diversity gain of the proposed MIMO antenna with RSW is computed and presented
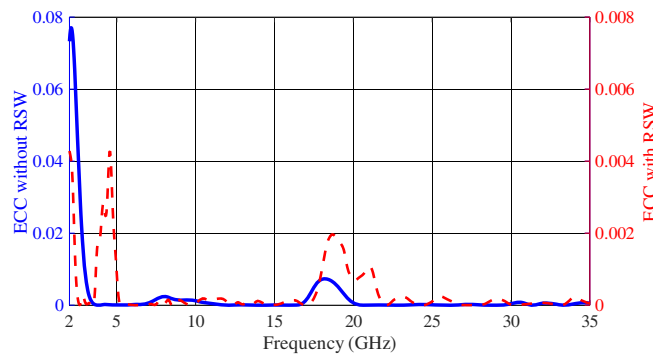

Figure 9. ECC of the MIMO antenna with RSW (red broken line) and without RSW (blue solid line).
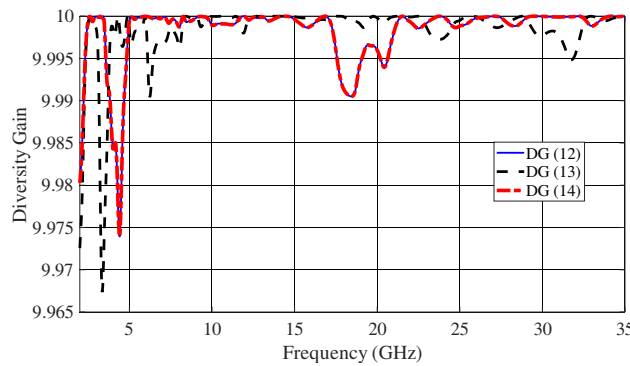

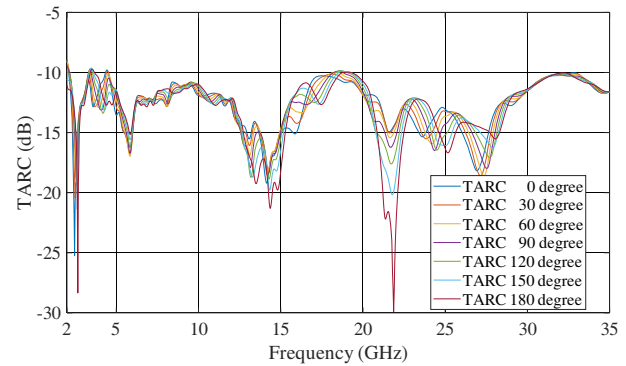**Figure 10.** Diversity gain of the MIMO antenna with RSW.

Figure 11. TARC of the MIMO antenna with RSW.

Table 2. Comparison with the reported typical counterparts.

Source	Planar Dimension (mm)	Bandwidth (GHz)	Isolation (dB)	Element numbers
Ref. [11]	48×48	3–11	-17	4
Ref. [12]	50×50	3–12	-16	4
Ref. [20]	85×50	2–9.5	20	2
Ref. [21]	22×33	2.9–12	15	2
Ref. [22]	50×30	2.5–14.5	20	2
Ref. [23]	70×70	24–14	18	4
Ref. [24]	40×40	2.86–4.9	-11	4
Ref. [25]	45×45	2.4–6	-14	4
This paper	32×32	2.2–30	-19	4

in Fig. 10. The diversity gain can be calculated using the following equation:

$$DG = 10\sqrt{1 - |\rho_e|^2} \qquad (2)$$

To predict the radiation performance of the MIMO antenna, the total active reflection coefficient (TARC) is computed. The TARC calculated can be directly from the scattering matrix by using the formula [27]:

$$\Gamma = \frac{\sqrt{\sum_{n=1}^{4} |S_{n1} + S_{n2}e^{j\theta} + S_{n3}e^{j\theta} + S_{n4}e^{j\theta}|^2}}{2} \qquad (3)$$

where $[b] = [S] \cdot [a]$. $[S]$ is the scattering matrix of the MIMO antenna, $[a]$ the excitation vector, and $[b]$ the scattered vector. Fig. 11 shows the calculated TARC with different values of theta. It can be seen that the TARC keeps under $-10\,\mathrm{dB}$ within the whole operation band.

5. CONCLUSION

In this paper, a compact quad-element MIMO antenna is developed based on our simulation study and measurement. The incorporation of a novel RSW structure in the antenna has makes it possible to achieve a high isolation between the antenna elements with low profile (3.5 mm) and wide bandwidth (2.2–7 GHz). Compared with other counterparts reported, the proposed quad-element MIMO antenna with four RSWs has a much smaller size (32 mm × 32 mm × 4.5 mm), wider operation bandwidth (2.2 GHz–30 GHz), and higher isolation (under $-19\,\mathrm{dB}$). The experimental results clearly indicate that the quad-element MIMO antenna with four RSWs is promising for the future 5G communication.

ACKNOWLEDGMENT

REFERENCES

1. Niu, Y., Y. Li, D. Jin, L. Su, and A. V. Vasilakos, "A survey of millimeter wave (mm Wave) communications for 5G: Opportunities and challenges," *Wireless Networks*, Vol. 21, No. 8, 2657–2676, Nov. 2015.
2. "Microwave towards 2020: Delivering high-capacity and cost-efficient backhaul for broadband networks today and in the future," Ericsson, Sep. 2015.
3. Rappaport, T. S., et al., "Millimeter wave mobile communications for 5G cellular: It will work!," *IEEE Access*, Vol. 1, 335–349, May 2013.
4. Roh, W., et al., "Millimeter-wave beamforming as an enabling technology for 5G cellular communications: Theoretical feasibility and prototype results," *IEEE Communications Magazine*, Vol. 52, No. 2, 106–113, Feb. 2014.
5. Rappaport, T. S., et al., "Overview of millimeter wave communications for Fifth-Generation (5G) wireless networks-with a focus on propagation models," *IEEE Trans. Antennas Propag.*, Vol. PP, No. 99, 1–1, Aug. 2017.
6. Park, J. S., et al., "A tilted combined beam antenna for 5G communications using a 28-GHz band," *IEEE Antennas Wireless Propag. Lett.*, Vol. 15, 1685–1688, Jan. 2016.
7. Li, M., et al., "Eight-port orthogonally dual-polarized antenna array for 5G smartphone applications," *IEEE Trans. Antennas Propag.*, Vol. 64, No. 9, 3820–3830, Sep. 2016.
8. Ge, L., et al., "Polarization-reconfigurable magnetoelectric dipole antenna for 5G Wi-Fi," *IEEE Antennas Wireless Propag. Lett.*, Vol. 16, 1504–1507, Jan. 2017.

9. Dadgarpour, A., et al., "Mutual coupling reduction in dielectric resonator antennas using metasurface shield for 60-GHz MIMO systems," *IEEE Antennas Wireless Propag. Lett.*, Vol. 16, 477–480, Mar. 2017.

10. Farahani, M., et al., "Mutual coupling reduction in millimeter-wave MIMO antenna array using a metamaterialpolarization-rotator wall," *IEEE Antennas Wireless Propag. Lett.*, Vol. 16, 2324–2327, Aug. 2017.

11. Mao, C. and Q. Chu, "Compact coradiator UWB-MIMO antenna with dual polarization," *IEEE Trans. Antennas Propag.*, Vol. 62, No. 9, 4474–4480, Sep. 2014.

12. Zhu, J., S. Li, B. Feng, L. Deng, and S. Yin, "Compact dual-polarized UWB quasi-self-complementary MIMO/diversity antenna with band-rejection capability," *IEEE Antennas Wireless Propag. Lett.*, Vol. 15, 905–908, Sep. 2015.

13. Gopikrishna, M., D. D. Krishna, C. K. Anandan, P. Mohanan, and K. Vasudevan, "Design of a compact semi-elliptic monopole slot antenna for UWB systems," *IEEE Trans. Antennas Propag.*, Vol. 57, No. 6, 1834–1837, Jun. 2009.

14. Rajesh, D., P. K. Sahu, and S. K. Behera, "A compact UWB parasitic microstrip antenna with band dispensation," *2011 Int. Conf. Devices Commun.*, 1–5, Mesra, India, Feb. 2011.

15. Yu, C., W. Hong, L. Chiu, G. Zhai, C. Yu, W. Qin, and Z. Kuai, "Ultrawideband printed log-periodic dipole antenna with multiple notched bands," *IEEE Trans. Antennas Propag.*, Vol. 59, No. 3, 725–732, Dec. 2010.

16. Jahromi, M. N., "Novel wideband planar fractal monopole antenna," *IEEE Trans. Antennas Propag.*, Vol. 56, No. 12, 3844–3849, Dec. 2008.

17. Rahman, M. U., D.-S. Ko, and J.-D. Park, "A compact multiple notched ultra-wide band antenna with an analysis of the CSRR-TO-CSRR coupling for portable UWB applications," *Sensors*, Vol. 17, No. 10, 2174, 2018.

18. Rahman, M. U., W. T. Khan, and M. Imran, "Penta-notched UWB antenna with sharp frequency edge selectivity using combination of SRR, CSRR, and DGS," *Int. J. Electron. Commun.*, Vol. 93, 116–122, Jun. 2018.

19. Zhao, X., S. P. Yeo, and L. C. Ong, "Planar UWB MIMO antenna with pattern diversity and isolation improvement for mobile platform based on the theory of characteristic modes," *IEEE Trans. Antennas Propag.*, Vol. 66, No. 1, 420–425, Jan. 2018.

20. Zhao, X., S. P. Yeo, and L. C. Ong, "Decoupling of inverted-F antennas with high-order modes of ground plane for 5G mobile MIMO platform," *IEEE Trans. Antennas Propag.*, Vol. 66, No. 9, 4485–4495, Sep. 2018.

21. Li, W., Y. Hei, P. M. Grubb, X. Shi, and R. T. Chen, "Compact inkjet-printed flexible MIMO antenna for UWB applications," *IEEE Access*, Vol. 6, 50290–50298, Sep. 2018.

22. Iqbal, A., O. A. Saraereh, A. W. Ahmad, and S. Bashir, "Mutual coupling reduction using F-shaped stubs in UWB-MIMO antenna," *IEEE Access*, Vol. 6, 2755–2759, Feb. 2018.

23. Saad, A. A. R., "Approach for improving inter-element isolation of orthogonally polarised MIMO slot antenna over ultra-wide bandwidth," *Electro. Lett.*, Vol. 54, No. 18, 1062–1064, Sep. 2018.

24. Sarkar, D. and K. V. Srivastava, "A compact four-element MIMO/diversity antenna with enhanced bandwidth," *IEEE Antennas Wireless Propag. Lett.*, Vol. 16, 2469–2472, May 2017.

25. Anitha, R., P. V. Vinesh, K. C. Prakash, P. Mohanan, and K. Vasudevan, "A compact quad element slotted ground wideband antenna for MIMO applications," *IEEE Trans. Antennas Propag.*, Vol. 64, No. 10, 4550–4553, Jul. 2016.

26. Hallbjörner, P., "The significance of radiation efficiencies when using S parameters to calculate the received signal correlation from two antennas," *IEEE Antennas Wireless Propag. Lett.*, Vol. 4, 97–99, Jun. 2005.

27. Chae, S. H., S. Oh, and S.-O. Park, "Analysis of mutual coupling, correlations, and TARC in WiBro MIMO array antenna," *IEEE Antennas Wireless Propag. Lett.*, Vol. 6, 122–125, Feb. 2007.